NANOSTRUCTURED SYNTHETIC OPAL-C

M. HERNÁNDEZ-ORTIZ[a,b], G. HERNÁNDEZ-PADRÓN[c1], R. BERNAL[d], C. CRUZ-VÁZQUEZ[b], M. VEGA-GONZÁLEZ[c2] AND V. M. CASTAÑO[C3,*].
Programa de Posgrado en Ciencia de Materiales[a] del Departamento de Investigación en Polímeros y Materiales, Universidad de Sonora, A. P. 130, Hermosillo, Sonora 83000 México[b], Departamento de Nanotecnología[c1], Centro de Física Aplicada y Tecnología Avanzada; Centro de Geociencias[c2]; Departamento de Ingeniería Molecular de Materiales[c3], Centro de Física Aplicada y Tecnología Avanzada; Universidad Nacional Autónoma de México, Campus Juriquilla, Boulevard Juriquilla No. 3001, Juriquilla, Querétaro, C.P. 76230, Departamento de Investigación en Física, Universidad de Sonora, A. P. 5-088, Hermosillo, Sonora 83190 México[d].

Nanocrystalline opal-C has been synthesized, through sedimentation and fast drying. The formation of spherical silica nanoparticles was studied using X-ray diffraction (XRD), infrared spectroscopy (FTIR) and scanning electron microscopy (SEM). Its crystallite size is calculated using Scherrer equation and Guthrie equation (modeled through XRD patterns of several very pure opal samples). SEM shows nano-sized particles in the 60-90 nm diameter range. The results are compared with a natural opal-CT the so-called 'fire opal'.

1. Introduction

Opal is an either amorphous or poorly-crystallized variety of silica that also contains water. Indeed, very little attention has been paid to the structure of gem opal varieties which do not exhibit play-of-color of common opal, as opal-C, which is a well ordered form of the silicate, predominantly in the α-cristobalite form. However, one of more studied materials of this family is fire opal located in many sites around the world, mainly Mexico. It is presented as opal-CT (for disordered α-cristobalite with α-tridymite-type stacking) and it is typically of volcanic origin. By contrast, play-of-color or noble opal is most known as opal-A (for amorphous), which is generally of sedimentary origin and its classical localities are Australia and the Piaui State of Brazil [1-8].

Early contributions made by Flörke (1955) based on XRD indicate that opals are disordered intergrowths of cristobalite and tridymite and Jones et al. (1964) determined that gem-quality opals are 3-dimensional arrays of amorphous silica spheres [3-5, 8-11]. Moreover, powder XRD remains the most commonly used technique to investigate opal, yet interpretations of opal XRD patterns still are largely qualitative [5].

On the other hand, the structures that display a regular three-dimensional stacking of silica spheres with voids in between them, lead to diffraction of visible light for the appropriate sphere diameter (about 150–300 nm), it has led to the development of the field of photonic band-gap materials [1, 9]. A good example, as application of opal, of a three-dimensional photonic crystal is synthetic opal composed of close-packed monodisperse amorphous SiO_2 spheres with a diameter

---

*Corresponding author: castano@fata.unam.mx

that may vary from 100 to 1000 nm. When the size of SiO_2 spheres is varied, the photonic band-gap position for opals can be tuned in a wide spectral range from ultraviolet to near infrared [10].

Characterization of photonic materials based on a synthetic opal performed by scattering matrix method is widely investigated [10, 12-20]. Moreover, reports of morphologic and structural properties are realized for microcrystalline opals [3, 21]. The purpose of this study is to analyze the crystal structure of synthetic opals of type C, developed by sedimentation method with particle sizes smaller that 100 nm, and to estimate their crystallite size.

2. Materials and methods

Opal samples were synthesized by Stöber method [22], consisting in the hydrolysis of tetraethyl-ortho-silicate (TEOS) using NH_3 as a catalyst and ethanol and acetone as solvents. The reaction was controlled in a Nalgene glass flask at room temperature. Synthetic opals underwent two thermal treatments aimed at strengthening the structure. First annealing was fixed at 1000 °C for one day and second thermal treatment was given at 1150 °C for two days. According to the report of Beganskienė [12], the solution (TEOS, NH_3, H_2O and solvent) chemistry controls the reaction rate and particle size. In this case, two batch of synthetic opals were obtained with different particle size (< 100 nm) characteristic from reaction mixtures of solvent: acetone (opal Oa) and ethanol (opal Oe).

FTIR absorption spectra of the powdered opal samples were obtained with a Perkin-Elmer Spectrum GX using the KBr pellet method. The SEM elaboration was performed using a JEOL JSM-6060LV microscope at magnifications up to x50 000 and operating at 30 kV. All samples, on a fresh break, were coated by a film of gold.

The opal structure is analyzed by XRD patterns of the samples produced, using a Rigaku diffractometer, model Miniflex. Operating conditions were Cu Kα radiation, 30 kV, 15 mA, resolution 0.02 degree and an interval of record $2\theta = 5.0–80.0°$. The crystallite size (L) was estimated on observed opals with the linear regression equation of full-width high-maximum (FWHM) to 1/L, with units of degrees two-theta and nanometers, used by Guthrie [23]. It is compared with the Scherrer equation, which constant (K) value of 0.907 and incident beam wavelength (λ), corresponding to the target, is 1.54 Å. Both are shown in equations 1 and 2, respectively.

$$L = \frac{8.78}{FWHM + 0.024}$$

(1)

$$FWHM = \frac{K\lambda}{L\cos\theta}$$

(2)

Also, methodology above was done on fire opals from deposits in Mexico, from the State of Queretaro (mina Cerro Viejo near San Juan del Rio). All measurements were carried out on powdered samples.

3. Results and discussion

The FTIR spectra of all samples are illustrated in figure 1. The typical IR spectrum of opal-CT is the same as displayed by natural sample, figure 1(a), absent in absorbance of the bands at 620 and 390 cm^{-1} which are characteristic for low-cristobalite. These are clearly visible in the spectra of opal-C, as it is presented in figure 1 (b) and (c) respectively of synthetic specimens [3-4]. Furthermore, the remaining broad bands near 1100, 790, and 480 cm^{-1} are common to all silicates with tetrahedrally coordinated silicon [24]. There is very little difference between the IR absorption spectra of the various forms of silica. However, the synthetic opal obtained does not present quartz, which is revealed by the distinctive absorption band in 695 cm^{-1} [4].
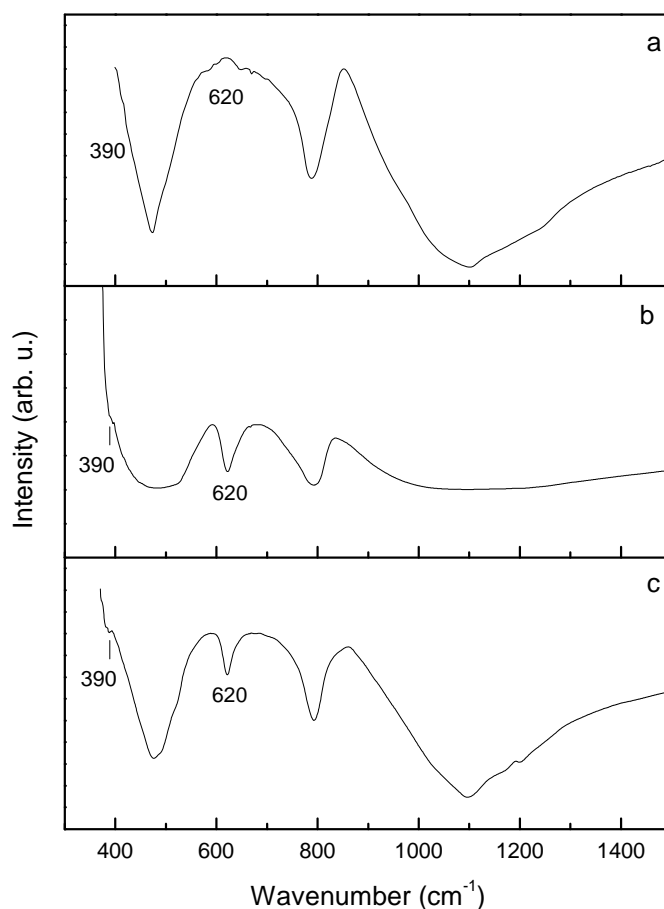
Fig. 1. Infrared absorption spectra of fire opal (a) and artificial opals from reaction mixtures of solvent: acetone (b) and ethanol (c).

The XRD patterns of all specimens show in particular a broad peak at ~19 - 24° 2θ and a peak at ~ 36° 2θ dominant features of the opal-CT [23], which are illustrated in figure 2. However, opal-C is known from the X-ray data to be a rather well-ordered α-cristobalite, but it is not appropriate to refer to this material as α-cristobalite because all diffraction patterns show evidence of tridymitic stacking, as it shows the strongest reflection through an additional shoulder for ~36° 2θ [11]. Hence, the main criteria to distinguish opal-CT from opal-C are the position and the width of the most intense Bragg reflection. Opal-CT exhibits broader Bragg reflections and the FWHM of the major peak in 2θ units is > 5.6° [25]. Therefore, it proves that synthetic opals of this work are opal-C as it is displayed in figure 2 (b and c) and the diffraction pattern of opal-CT confirms the structure of fire opal, figure 2 a.
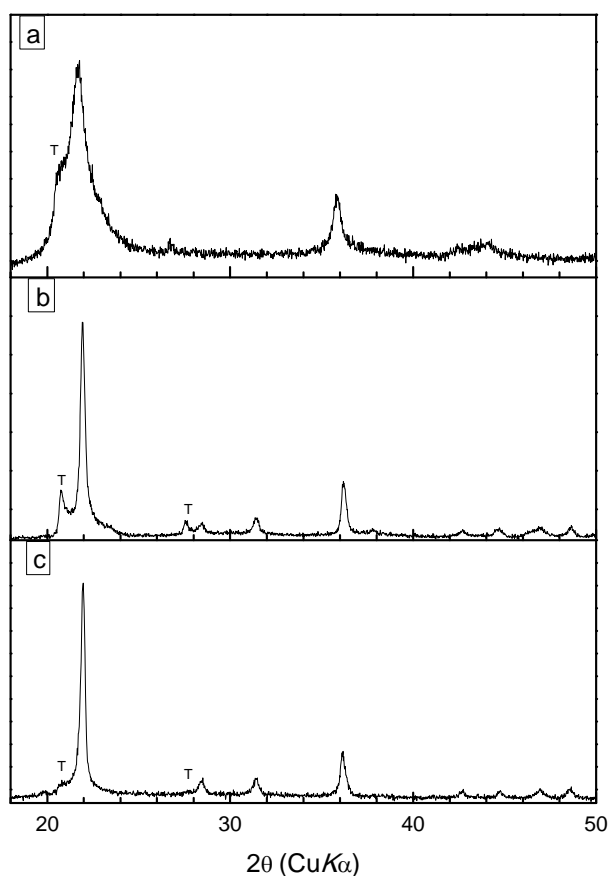
Fig. 2. XRD pattern for fire opal or opal-CT, image (a), and X-ray powder diagrams of synthetic opals: Oa (b) and Oe (c), both indicated to be opal-C. Peaks marked T to tridymitic stacking.

FWHM of the ~36° 2θ peak is primarily sensitive to the size of the opal crystallites. Equation 1 was computed using the XRD patterns of several very pure opal samples [23]. This equation is compared with the Scherrer equation (equation 2), method recognized to determine crystallite size using the diffraction technique. Table 1 displays the crystallite size of the synthetic opals and fire opal given by equations 1 and 2. In both methods, natural opal presents a crystallite size lower than synthetic opals. The range for the crystallite sizes of the opals studied , determined by Guthrie method, is 18-27 nm, and is in agreement with the range of crystallite sizes calculated on different opal-CT samples using TEM, of 12-32 nm [26]. This interval is less than that given by Scherrer equation, 31-38 nm, where only fire opal enters in the same report. This equation shows crystallite size values highest, for Oa and Oe opal, both with structure type as opal-C. In this case, crystallite size between Oa and Oe opal preserve order with respect to synthesis publication of silica nanoparticles [12].

***Error! Reference source not found.**. Crystallite size (L) of synthetic and natural opals determined by e*

Sample	FWHM (° 2θ)	L (nm)	
		Guthrie (eq. 1)	Scherrer (eq. 2)
Oa	0.30	27.10	38.13
Oe	0.36	22.86	31.47
Fire opal	0.46	18.14	30.98
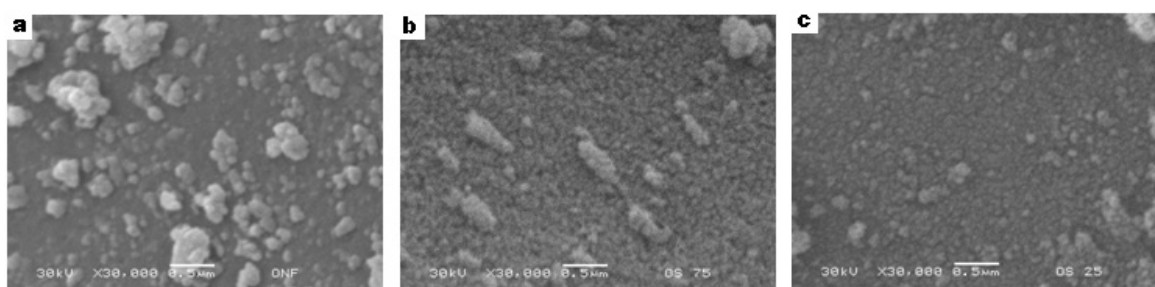
Fig. 3. SEM images of the natural opal (a) and synthetic opals: Oa (b) and Oe (c).

Fig. 3 shows the SEM micrographs of silica spheres correspondent to each studied samples. Synthetic opals present a space visible between spherical grains to low contrast, in spite of specimen preparation being on a fresh break and magnification used of x50 000. This differs from what happens in the fire opal case, as depicted in the bright areas in figure 3c, where there are present major random aggregates of nanometer sized particles. The boundaries between nanograins are very convoluted and could be artifacts of the preparation method [1]. However, individual particles size observed in these opals is measured. About 84 nm in size on average is corresponding to the natural opal and Oe and Oa opal have 67 and 90 nm mean sizes, respectively. Despite particle size is based in spheres overlooking in the image, artificial opals present a grain mean size according with the crystallite size order.

The particle size of synthetic opals, shown by SEM, does not match with the particle size reported by Beganskienė [12], for the case of opal Oe. The synthesis process utilized presents important variations, mainly related to the drying speed and thermal treatment. This causes a rearrangement of particles that can lead to the apparition of agglomerates which are observed in SEM. Synthetic opals have different particle sizes, which do not lead to significant differences in the FTIR spectra. Moreover, XRD patterns show that opal Oa has more structural elements of tridymite than opal Oe (lower particle size), as displayed in Figure 2 b and c by additional shoulders on the 19.5-24.50 2θ peak, which correspond to the strongest reflections in a powder diagram of tridymite [3].

4. Conclusion

This work contributes to the study of the nanostructure of a specific synthetic opal, opal-C, obtained by the sedimentation method with a thermal treatment relatively fast, that could to be used as photonic material. X-ray powder diffractograms and infrared absorption bands confirm that synthetic and natural samples present a structure-type opal-C and opal-CT, respectively. FTIR spectra display features of opal absorption bands with tetrahedrally coordinated silicon. Also,

crystallite size of opals studied was calculated using two equations, Scherrer equation and Guthrie equation. Opals crystallite size estimated by Guthrie equation confirms the data already reported. Interestingly, the two calculation methods showed that synthetic opal has larger crystallite size than natural opal-CT. SEM micrographs of synthetic opals C-type exhibit ordered sequences of the particles array, and in contrast, the fire opal presents major number of cluster.

Acknowledgement

References

[1] E. Fritsch, E. Gaillou, B. Rondeau, A. Barreau, D. Albertini, M. Ostroumov, Journal of Non-Crystalline Solids. **352**, 3957 (2006).
[2] A.G. Smallwood, P.S. Thomas, A.S. Ray, Spectrochimica Acta Part A. **53**, 2341 (1997).
[3] H. Graetsch, H. Gies, I. Topalovi, Phys. Chem. Minerals. **21**, 166 (1994).
[4] J.B. Jones, E.R. Segnit, Australian Journal of Earth Sciences. **18**, 57 (1971).
[5] G.D. Guthrie, Jr., D.L. Dish, R.C. Reynolds, Jr., American Mineralogist. **80**, 869 (1995).
[6] E.R. Segnit, C.A. Anderson, J.B. Jones, Search, **1**, 349 (1970).
[7] A. Ilieva, B. Mihailova, Z. Tsintsov, O. Petrov, American Mineralogist. **92**, 1325 (2007).
[8] E. Fritsch, E. Gaillou, M. Ostroumov, B. Rondeau, B. Devouard, A. Barreau, Eur. J. Mineral. **16**, 743 (2004).
[9] M. Ostrooumov, E. Fritsch, S. Lefrant, Revista Mexicana de Ciencias Geológicas. **16**, 73 (1999).
[10] V.G. Golubev, J.L. Hutchison, V.A. Kosobukin, D.A. Kurdyukov, A.V. Medvedev, A.B. Pevtsov, J. Sloan, L.M. Sorokin, Journal of Non-Crystalline Solids. **299**, 1062 (2002).
[11] J.B. Jones, J.V. Sanders, E.R. Segnit, Nature. **204**, 990 (1964).
[12] A. Beganskienė, V. Sirutkaitis, M. Kurtinaitienė, R. Juškėnas, A. Kareiva, Materials Science (Medžiagotyra). **10**, 287 (2004).
[13] L. Pallavidino, D. Santamaria Razo, F. Geobaldo, A. Balestreri, D. Bajoni, M. Galli, L.C. Andreani, C. Ricciardi, E. Celasco, M. Quaglio, F. Giorgis, Journal of Non-Crystalline Solids. **352**, 1425 (2006).
[14] E.J. Nassar, K.J. Ciuffi, R.R. Gonçalves, Y. Messaddeq, S.J.L. Ribeiro, Quim. Nova. **26**, 674 (2003).
[15] A. Xiang, J.P. GAO, H.K. Chen, J.G. Yu, R.X. Liu, Chinese Chem. Lett. **15**, 228 (2004).
[16] J. F. Galisteo-López, E. Palacios-Lidón, E. Castillo-Martínez, C. López, Phys. Rev. B. **68** (2003) id. 115109.
[17] H. Miguez, N. Tétreautl, S.M. Yang, V. Kitaev, G.A. Ozin, Adv Mater. **15**, 597 (2003).
[18] F. García-Santamaria, C. López, F. Meseguer, P.V. Braun, Adv Mater. **15**, 788 (2003).
[19] A. Reynolds, F. López-Tejeira, D. Cassagne, F. J. García-Vidal, C. Jouanin, J. Sánchez-Dehesa, Physical Review B. **60**, 11422 (1999).
[20] A. Balestreri, L.C. Andreani, M. Agio, Physical Review E. **74**, 036603 (2006).
[21] S.L. Cady, H.R. Wenk, Geological Society of America Abstracts with Programs. **26**, A112 (1994).
[22] W.Stöber, A. Fink, E. Bohn, Journal of Colloid and Interface Science. **26**, 62 (1968).
[23] G.D. Guthrie, Jr., D. L. Bish, R.C. Reynolds, Jr., American Mineralogist. **80**, 869 (1995).
[24] M. Ostrooumov. Spectrochimica Acta Part A. **68**, 1070 (2007).
[25] A. Ilieva, B. Mihailova, Z. Tsintsov, O. Petrov, American Mineralogist. **92**, 1325 (2007).
[26] S.B. Rice, J.M. Elzea, Society Annual Meeting Abstracts with Program, 137, (1993).